

Topological Solitons and Folded Proteins

M.N. Chernodub,^{1,2,*} Shuangwei Hu,^{1,3,†} and Antti J. Niemi^{3,1,‡}

¹*Laboratoire de Mathématiques et Physique Théorique, Université François-Rabelais Tours,
Fédération Denis Poisson - CNRS, Parc de Grandmont, 37200 Tours, France*

²*Department of Mathematical Physics and Astronomy, Krijgslaan 281, 59, Gent, B-9000, Belgium*

³*Department of Physics and Astronomy, Uppsala University, P.O. Box 803, S-75108, Uppsala, Sweden*
(Dated: February 4, 2022)

We propose that protein loops can be interpreted as topological domain-wall solitons. They interpolate between ground states that are the secondary structures like α -helices and β -strands. Entire proteins can then be folded simply by assembling the solitons together, one after another. We present a simple theoretical model that realizes our proposal and apply it to a number of biologically active proteins including 1VII, 2RB8, 3EBX (Protein Data Bank codes). In all the examples that we have considered we are able to construct solitons that reproduce secondary structural motifs such as α -helix-loop- α -helix and β -sheet-loop- β -sheet with an overall root-mean-square-distance accuracy of around 0.7 Ångström or less for the central α -carbons, *i.e.* within the limits of current experimental accuracy.

PACS numbers: 87.15.A-, 87.15.Cc, 87.14.hm

Solitons are ubiquitous and widely studied objects that can be materialized in a variety of practical and theoretical scenarios [1], [2]. For example solitons can be deployed for data transmission in transoceanic cables, for conducting electricity in organic polymers [1], and they may also transport chemical energy in proteins [3]. Solitons explain the Meissner effect in superconductivity and dislocations in liquid crystals [1]. They also model hadronic particles, cosmic strings and magnetic monopoles in high energy physics [1] and so on. The first soliton to be identified is the Wave of Translation that was observed by John Scott Russell in the Union Canal of Scotland. This wave can be accurately described by an exact soliton solution of the Korteweg-de Vries (KdV) equation [1]. At least in principle it can also be constructed in an atomary level simulation where one accounts for each and every water molecule in the Canal, together with all of their mutual interactions. However, in such a *Gedanken* simulation it would probably become a real challenge to unravel the collective excitations that combine into the Wave of Translation without any guidance from the known soliton solution of the KdV equation since solitons can *not* be constructed simply by adding up small perturbations around some ground state: A (topological) soliton emerges when non-linear interactions combine elementary constituents into a localized collective excitation that is stable against small perturbations and cannot decay, unwrap or disentangle [1], [2].

In this Letter we propose that (topological) solitons can also explain and describe the folding of proteins into their native state [4], [6]. We characterize a folded protein by the Cartesian coordinates \mathbf{r}_i of its N central α -carbons, with $i = 1, \dots, N$. For many biologically active proteins these coordinates can be downloaded from Protein Data Bank (PDB) [7]. Alternatively, the protein can be described in terms of its bond and torsion angles that

can be computed from the PDB data. For this we introduce the tangent vector \mathbf{t}_i and the binormal vector \mathbf{b}_i

$$\mathbf{t}_i = \frac{\mathbf{r}_{i+1} - \mathbf{r}_i}{|\mathbf{r}_{i+1} - \mathbf{r}_i|} \quad \& \quad \mathbf{b}_i = \frac{\mathbf{t}_{i-1} \times \mathbf{t}_i}{|\mathbf{t}_{i-1} \times \mathbf{t}_i|} \quad (1)$$

Together with the normal vector $\mathbf{n}_i = \mathbf{b}_i \times \mathbf{t}_i$ we then have three vectors that are subject to the discrete Frenet [8] equation

$$\begin{pmatrix} \mathbf{n}_{i+1} \\ \mathbf{b}_{i+1} \\ \mathbf{t}_{i+1} \end{pmatrix} = \exp\{-\kappa_i \cdot T^2\} \cdot \exp\{-\tau_i \cdot T^3\} \begin{pmatrix} \mathbf{n}_i \\ \mathbf{b}_i \\ \mathbf{t}_i \end{pmatrix} \quad (2)$$

Here T^2 and T^3 are two of the standard generators of three dimensional rotations, explicitly in terms of the permutation tensor we have $(T^i)^{jk} = \epsilon^{ijk}$. From (1), (2) we can compute the bond angles κ_i and the torsion angles τ_i using PDB data for \mathbf{r}_i . Alternatively, if we know these angles we can compute the coordinates \mathbf{r}_i . The common convention is to select the range of these angles so that κ_i is positive. In the continuum limit where (2) becomes the standard Frenet equation for a continuous curve, $\kappa_i \rightarrow \kappa(x)$ then corresponds to local curvature.

As an example we consider the 35 residue villin head-piece protein with PDB code 1VII that has been widely investigated, both theoretically and experimentally [4]. For example in the state of the art simulation [5] succeeded in producing its fold for a short time within an accuracy of $\sim 2 - 3\text{Å}$.

From the PDB data we compute the values of bond angles κ_i and torsion angles τ_i and the result is displayed in Figure 1(a), where we use the (standard) convention that the discrete Frenet curvature κ is positive. In 1VII there are three α -helices that are separated by two loops. When we use the PDB (NMR) convention for indexing the residues the first, longer, loop is located at sites 49-54 and the second, shorter, between 59-62.

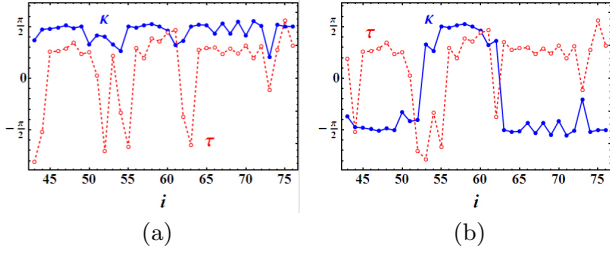


FIG. 1: (a) The bond and torsion angles of 1VII, computed with the (standard) convention that the discrete Frenet curvature κ is positive. (b) The \mathbb{Z}_2 gauge transformed bond and torsion angles.

We shall now show that Figure 1(a) describes two soliton configurations, albeit in an encrypted form. In order to decrypt the data in Figure 1(a) so that these solitons become unveiled we observe that the equation (2) has the following local \mathbb{Z}_2 gauge symmetry: At every site we can send

$$\mathbb{Z}_2 : \begin{cases} \kappa_i \rightarrow \kappa_i \cdot \cos(\Delta_{i+1}) \\ \tau_i \rightarrow \tau_i + \Delta_i - \Delta_{i+1} \end{cases} \quad (3)$$

and when we choose at each site $\Delta_i = 0$ or $\Delta_i = \pi$ where $\Delta_i = \pi$ is the nontrivial element of the \mathbb{Z}_2 gauge group, the Cartesian coordinates \mathbf{r}_i computed from the discrete Frenet equation remain intact. If we judiciously implement this \mathbb{Z}_2 gauge transformation in the data displayed in Figure 1(a) we arrive at the apparently quite different Figure 1(b). Unlike in Figure 1(a), the profile of κ_i in Figure 1(b) clearly displays the hallmark profile of a topological soliton-(anti)soliton pair in a double-well potential: The two solitons are located around the sites with indices 49-54 and 59-62 which are the locations of the two loops in 1VII. These solitons interpolate between the two "ground state" values $\kappa_i \approx \pm\pi/2$ that pinpoint the locations of the α -helices in 1VII. Moreover, the two downswings in the value of τ_i from the value $\tau_i \approx 1$ that mark the locations of the α -helices, coincide with the locations of the two solitons. The ensuing combined profile of κ_i and τ_i is qualitatively consistent with a double-well potential structure in the (κ, τ) plane that has the form displayed in Figure 2: When we move from left to right in Figure 1(b), we follow a trajectory in the (κ, τ) plane that starts by fluctuating around the potential energy minimum at $(\kappa, \tau) \approx (-\pi/2, 1)$ in Figure 2, corresponding to the first α -helix. The trajectory then moves through the first loop *a.k.a.* soliton (the red dashed line) to the second potential energy minimum *i.e.* α -helix at $(\kappa, \tau) \approx (+\pi/2, 1)$ in Figure 2, and finally back through the second loop *a.k.a.* soliton (the blue solid line) to the first potential energy minimum at $(\kappa, \tau) = (-\pi/2, 1)$. We now present a simple theoretical model [9], [10] that reproduces the (κ, τ) profile in Figure 1(b) as a combination of two soliton solutions, with a very high atomary level accuracy for the central α -carbons. The model is

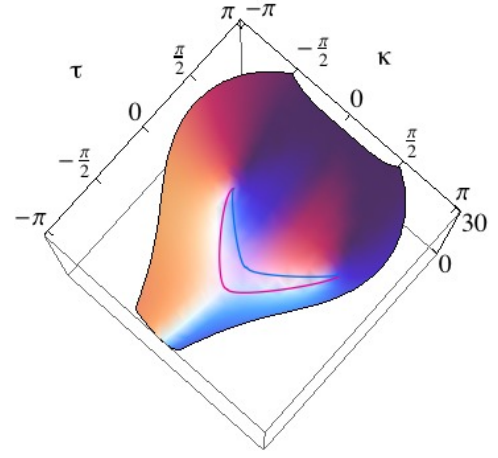


FIG. 2: The potential energy on (κ, τ) plane that corresponds qualitatively to the data in Figure 1(b), the soliton between sites 49-54 corresponds to the red dashed trajectory and the soliton between sites 59-62 to the blue solid trajectory.

defined by the energy functional

$$E = \sum_{i=1}^{N-1} (\kappa_{i+1} - \kappa_i)^2 + \sum_{i=1}^N c \cdot (\kappa_i^2 - m^2)^2 + \sum_{i=1}^N \{b \kappa_i^2 \tau_i^2 + d \tau_i + e \tau_i^2 + q \kappa_i^2 \tau_i\} \quad (4)$$

Here N is the number of central α -carbons and (c, m, b, d, e, q) are parameters. The first sum describes nearest neighbor interactions along the protein. The second sum describes a local self-interaction of the bond angles. The third sum describes local interactions between bond and torsion angles, its first term has an origin in a Higgs effect which is due to the potential term in the second sum. The second term in the third sum is the Chern-Simons term, it is responsible for the chirality of the protein chain. The third term is a Proca mass term and the last term can also be related to the Abelian Higgs Model, and it is also chiral. As explained in [10] this energy functional is essentially unique, and in particular it can be related to a gauge invariant (supercurrent) version of the energy of 1+1 dimensional lattice Abelian Higgs Model. In three space dimensions this model is also known as the Ginzburg-Landau Model of conventional superconductivity [2]. Note that in (4) there is no reference to the specifics of the interactions involving amino acids such as hydrophobic, hydrophilic, long-range Coulomb, van der Waals, saturating hydrogen bonds *etc.* interactions that are presumed to drive the folding process. The only explicit long-range force present in (4) is the nearest neighbor interaction described by the first term. Moreover, as it stands (4) depends only on *six* site-independent, homogeneous parameters. There is no direct reference whatsoever to the underlying in general

highly inhomogeneous amino acid structure of a protein. We argue that this becomes possible since (4) supports *solitons* that describe the common secondary structural motifs such as α -helix/ β -strand - loop - α -helix/ β -strand as solutions to its classical equations of motion. Furthermore, even though the actual numerical values of the parameters are certainly motif dependent and for long loops that constitute bound states of several solitons one might need to introduce more than six parameters, we expect there to be wide *universality* so that a given soliton with its relatively few parameters describes a general class of homologous motifs. Consequently only a relatively small set of parameters are needed to provide soliton templates for structure prediction. In fact, we propose that solitons are the mathematical manifestation of the experimental observation, that the number of different protein folds is surprisingly limited. The presence of solitons could then be the reason for the success of bioinformatics based homology modeling in predicting native folds [4]. In order to quantitatively disclose the soliton solution of (4) we start by observing that the first two sums in (4) can be interpreted as a discrete version of the energy of the 1+1 dimensional double well $\lambda\phi^4$ model that is known to support the topological kink-soliton. In the continuum limit the kink has the analytic form [1], [2],

$$\kappa(x) = m \cdot \tanh[m\sqrt{c} \cdot (x - x_0)].$$

We can try to estimate the parameters m and c for each of the two solitons in the Figure 1(b) by a least square fitting where we use this continuum soliton to approximate the exact soliton solution of the discrete equations of motion. We consider here explicitly only the first soliton of 1VII, located between (PDB index) sites 49-54. Using the sites 46-56 we find the following least square fit

$$\kappa(x) \approx 1.4627 \cdot \tanh[2.0816(x - 52.597)]. \quad (5)$$

In order to construct $\tau(x)$ we solve for its equation of motion in (4). The result is

$$\tau(x) \approx -2.4068 \cdot \frac{1 - 0.4689 \cdot \kappa^2(x)}{1 - 0.4619 \cdot \kappa^2(x)} \quad (6)$$

In Figure 3 we show how the data in Figure 1(b) is described by the approximate soliton profile (5), (6). When we construct the ensuing discrete curve in the three dimensional space by solving (2) with for κ_i and τ_i given by (5) and (6), we reproduce the first loop of 1VII with a surprisingly good RMSD accuracy of ~ 1.43 Å for the PDB indices 46-56 which is quite remarkable, taking into account the simplicity of our approximation.

In order to construct a more accurate description of 1VII, we resort to a numerical construction of a soliton solution to the equations of motion if (4). We use simulated annealing that involves a Monte Carlo energy

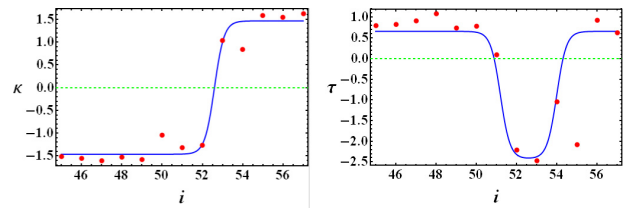


FIG. 3: The PDB data for the first α -helix - loop - α -helix motif in 1VII, on the left κ_i and on the right τ_i , together with the least square approximations (5) and (6) (the blue solid lines).

minimization of the energy functional

$$F = -\beta_1 \cdot \sum_{i=1}^N \left\{ \left(\frac{\partial E}{\partial \kappa_i} \right)^2 + \left(\frac{\partial E}{\partial \tau_i} \right)^2 \right\} - \beta_2 \cdot \sqrt{\frac{1}{N} \sum_{i=1}^N |\mathbf{r}_{\text{PDB}}(i) - \mathbf{r}_{\text{soliton}}(i)|^2} \quad (7)$$

with a simultaneous cooling of the two (inverse) temperatures β_1 and β_2 . Here the first sum vanishes when we have a solution to the classical difference equation of motion of (4), and the second sum computes the RMSD distance between the i th α -carbon of the solution and the protein we wish to construct. The second term in (7) acts like a chemical potential that selects the parameters in (4) so that we arrive at a soliton solution that corresponds to the given protein.

We have numerically constructed the classical solutions of (4) that describe the secondary structural motifs in proteins with PDB codes 1VII, 2RB8 and 3EBX. The first one has three α -helices separated by loops, while the second and third have β -strand-loop- β -strand motifs; Both cases can be described equally by (4), the only difference is that in the case of β -strands the two minima of the (classical) potential in (4) are located at $(\kappa, \tau) \approx (\pm 1, \pi)$. In each of the proteins that we have studied we have routinely been able to reproduce the secondary structural motifs as classical soliton solutions to the equations of motion for (4) in terms of only six parameters and with an overall RMSD accuracy of around 0.7 Å per motif which is essentially the experimental accuracy in X-ray crystallography and NMR; in our simulations the first sum in (7) decreases typically by around ten orders of magnitude indicating that the final configuration is a solution, essentially within numerical accuracy. Consequently at least in these proteins the secondary structural motifs can be viewed as solitons of the model (4), within experimental accuracy. Since the motifs that we have considered are quite generic in PDB data, we have very little doubt that our results will continue to persist whenever we have loops that connect α -helices and/or β -strands. And as long as the loops are not very long and do not describe bound states of several solitons there

does not appear to be any need to introduce more than six parameters. Work is now in progress to systematically construct and classify the solitons that describe the secondary structural motifs in a large class of biologically active proteins.

We have also made tentative attempts to use our solitons to reconstruct entire proteins, by *naively* joining the solitons that describe the secondary structural motifs at their ends. In the case of 1VII we have been able to reproduce in this manner the entire protein as a classical soliton with an overall RMSD accuracy of around 1.2 Å and the result is shown in Figure 4. Even though the

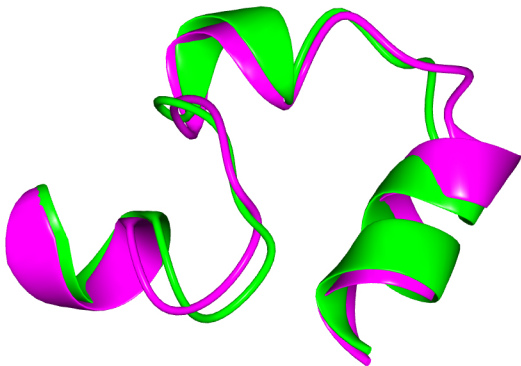


FIG. 4: The helix-loop-helix-loop-helix structure of the 1VII protein (green) together with its reconstruction in terms of two solitons (purple). The RMSD distance between the two configurations is ≈ 1.2 Å.

accuracy we obtain is very good, the loss of accuracy from ~ 0.7 Å to ~ 1.2 Å when we combine the two solitons suggests that we can still substantially improve the method of assembling an entire folded protein from its solitons. Work is now in progress to develop more efficient methods for assembling entire proteins from their solitons.

In conclusion, we have proposed that the common secondary structural motifs that describe loops connecting α -helices and/or β -strands can be interpreted as topological solitons, with the α -helices and β -sheets viewed as ground states that are interpolated by the loops as solitons. Entire proteins can then be assembled simply

by combining these solitons together one after another. We have also presented a model that allows us to fold proteins in terms of its solitons within experimental accuracy. In its simplest form that we have considered here, the model has only six site independent but in general motif dependent parameters. This appears to be sufficient to describe loops that are not too long. This observation that all the details and complexities of amino acids and their interactions can be summarized in so simple terms suggests the existence of wide universality in protein folding, and it can be viewed as a mathematically precise formulation of the experimental observation that the number of protein conformations is far more limited than the number of different amino acid combinations. Finally, we leave it as a future challenge to expand the model so that it incorporates an order parameter that describes the local orientation of the amino acids along the α -carbon backbone.

Our research is supported by grants from the Swedish Research Council (VR). We thank Martin Lundgren for discussions.

* On leave of absence from ITEP, Moscow, Russia; Electronic address: Chernodub@lmpt.univ-tours.fr

† Electronic address: Shuangwei.Hu@lmpt.univ-tours.fr

‡ Electronic address: Antti.Niemi@physics.uu.se

- [1] T. Dauxois and M. Peyrard, *Physics of Solitons* (Cambridge University Press, Cambridge, 2006)
- [2] N. Manton and P. Sutcliffe, *Topological Solitons* (Cambridge University Press, Cambridge, 2004)
- [3] A.S. Davydov, *Journ. Theor. Biology* **38**, 559 (1973).
- [4] K.A. Dill, S. Banu Ozkan, M.S. Shell and T.R. Weikl, *The Protein Folding Problem*, *Annual Review of Biophysics* **37**, 289 (2008)
- [5] G. Jayachandran, V. Vishal and V.S. Pane, *J. Chem. Phys.* **124**, 164902 (2006)
- [6] K. Huang, *Lectures On Statistical Physics And Protein Folding* (World Scientific Publishing Co. Pte. Ltd. Singapore, 2005)
- [7] H.M. Berman, K. Henrick, H. Nakamura and J.L. Markley, *Nucl. Acids Research* **35** (Database issue) D301-3 (2007)
- [8] P.J. Flory, *Statistical Mechanics of Chain Molecules* (Wiley, New York, 1969)
- [9] A. J. Niemi, *Phys. Rev. D* **67**, 106004 (2003) [arXiv:hep-th/0206227].
- [10] U.H. Danielsson, M. Lundgren and A.J. Niemi, e-print arXiv:0902.2920